Growth and characterization of DL-Norleucine maleate crystals

A. Z. Bazeera[a,*], D. Muthuraj[b], A. S. Mohamed[c], S. C. V. Durai[d], M. A. Nashrin[e]
[a]*Department of Physics, Sadakathullah Appa College, Tirunelveli, Tamilnadu, India*
[b]*Department of Physics, M.D.T.Hindu College, Tirunelveli, Tamilnadu, India*
[c]*Department of Chemistry, Sadakathullah Appa College, Tirunelveli, Tamilnadu, India*
[d]*Department of Physics, JP College of Arts & Science, Tenkasi, Tamilnadu, India*
[e]*Department of Physics, Sadakathullah Appa College, Tirunelveli, Tamilnadu, India, Affiliated to Manonmaniam Sundaranar University, Abishekapatti, Tirunelveli, Tamilnadu, India*

To obtain the single crystals of DL-Norleucine Maleate (DLNM), slow evaporation solution growth technique was used. The good crystalline quality of the crystal was validated by the diffraction peaks of the Powder X-Ray diffraction techniques. The functional groups which are present in the crystal were validated by FTIR and FT Raman method. Density functional theory (DFT) computation gives optimized structure parameters of DLNM molecule. The compound is changeless thermally up to 160°C and it is illustrated by TG-DTA thermal studies. The composition of the DLNM crystal was studied by EDAX spectroscopy. NMR spectral and chemical shifts of the grown crystal of DLNM were analyzed. The study of Vickers micro hardness study leads to the hardness number (H_V) evaluation and work hardening coefficient. Various dielectric parameters like AC conductivity, dielectric constant and loss energy of the sample were determined from the dielectric studies.

(Received November 29, 2021; Accepted March 28, 2022)

Keywords: Dielectric studies, DFT, EDAX, FT-IR, Norleucine naleate, Vickers micro hardness

1. Introduction

Organic compounds with large π- electron delocalization, in recent years, have attracted the interests of material scientists. The reason is their potentiality of applications in optical signal processing; optical communication. They frequently own exciting ferroelectric, ferromagnetic and superconducting properties, etc. [1]. Obtain the craved optical properties; the structures of organic materials can be modified easily. The hydroxyl groups of heterocyclic nitrogen atoms and carboxylic acids have be confirmed to a beneficial and effective organizing force contribution of supra molecules owing to its strongly hydrogen bonding [2-3]. Maleic acid is a dicarboxylic acid with chemical formula $HO_2CCHCHCO_2H$. The intermolecular hydrogen bond is strongly enough in maleic acid. Through hydrogen bonding and π-π interactions, crystalline maleates of various organic molecules are formed by it. As an acceptors to various various π-stacking complexes with other aromatic molecules, the maleic acid acts. Also, it acts as an acidic ligand for the formation of salts through determined electrostatic interaction [4]. DL- Norleucine is a synthetic amino acid which is of distinct interest because of its steric and structural similarities to the natural amino acid methionine [5]. It is hydrophobic, aliphatic and non-polar in nature. It has been used in various computational studies such as molecular dynamics simulations for elucidating the solid-state transition mechanism in molecular crystals [6-8]. In this work, DL-Norleucine maleate crystals are formed by slow evaporation method by mixing DL-Norleucine and maleic acid and its properties have been analyzed by various techniques.

* Corresponding author: meeran.jul1@gmail.com
https://doi.org/10.15251/JOR.2022.182.195

2. Experimentals

2.1. Synthesis DLNM crystal

DL-Norleucine Maleate (DLNM) was synthesized by taking DL-Norleucine (Hi-media) and Maleic acid (GR grade) in 1:1 stoichio-metric ratio. The reactants in total amounts were calculated and they are dissolved in stirred well and double distilled water thoroughly for 6 hours approximately. It is done with the help of a magnetic stirrer to make sure that thoroughly temperature and concentration are over the total volume of the solutions. Using a Whatsman filter paper of pore size 11 µm, the solution was filtered. It was transformed to crystal growth then, and under room temperature, crystallizations were permitted to happen by slow evaporation. The transparent colourless DLNM crystals, which were harvested in a period of 45-50 days, are illustrated in Fig.1.

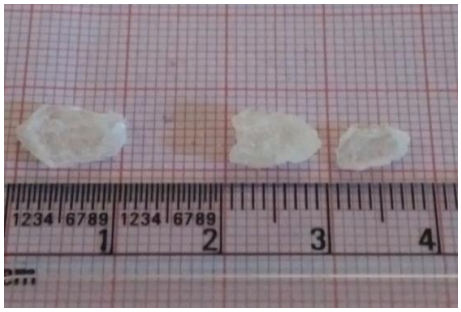

Fig. 1. Photograph of grown DLNM crystals.

2.2. Characterization techniques

Powder X-ray diffraction studies of DLNM were accomplished thoroughly. The samples, from 10^0 to 80^0 at a rate of 2^0per minute, were scanned for 2θ values. Density Functional Theoretical (DFT) computation studies were analyzed. The lattice dimensions of the grown specimen, using SHELX program, were derived from the single crystal XRD analysis. FTIR spectra of the grown crystals, in the range of 400 cm^{-1} to 4000 cm^{-1} using KBr pellet method on BRUKKER IFS FTIR spectrometer, were recorded. The Gaussian 09 suite with the DFT (density functional theory) was employed for the rate of impressing the ground state geometry of the sample and to get its theoretical FTIR and FT-Raman spectra. Differential Thermal Analysis (DTA) and Thermo-Gravimetric analysis (TG), using SDTQ 600 V8.2 (Universal V4.2 ETA) thermal analyzer in the temperature range 35- 600^o C for the grown crystal of DLNM to study the thermal stability, were accomplished simultaneously. Good quality and well-polished DLNM crystal was placed on the platform of the Vickers micro hardness tester. Loads of different magnitudes, with a view to examine the hardness crystal, were employed for a fixed interval of 10 seconds. EDAX or EDS spectroscopy is used to find the composition of the grown crystal of DLNM. The single crystal of DLNM, applying HIOKI 3532 LCR HITESSTER in the frequency range between 100 Hz and 5.5 MHz, was utilized for the dielectric measurement. The density of the grown crystal of DL-Norleucine Maleate crystals was measured by floatation method.

3. Results and discussion

3.1. Single crystal and powder XRD studies

The fine powder sample was subjected to powder XRD analysis. The presence of sharp peak in the XRD pattern denotes that good crystalline nature is shown in Fig. 2. The peaks at 16.95° and 22.48° confirms the presence of amino acid leucine group [9,10]. It is noticed from the single crystal XRD studies that the grown crystal of DLNM crystallizes in monoclinic structure with space group of $P2_1$ with cell parameters a = 28.731 Å, b= 6.734 Å, c = 11.732 Å, α=90^o,

β=99.42°, γ = 90°. The volume of the unit cell is 2239.23 Å^3. The molecular structure of DLMN crystal is shown in Fig. 3.

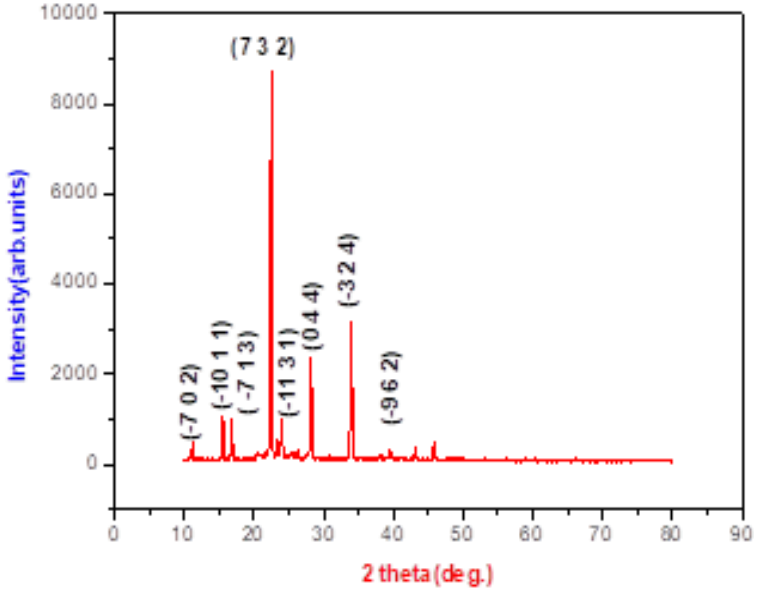

Fig. 2. Powder XRD pattern of DLNM crystal.

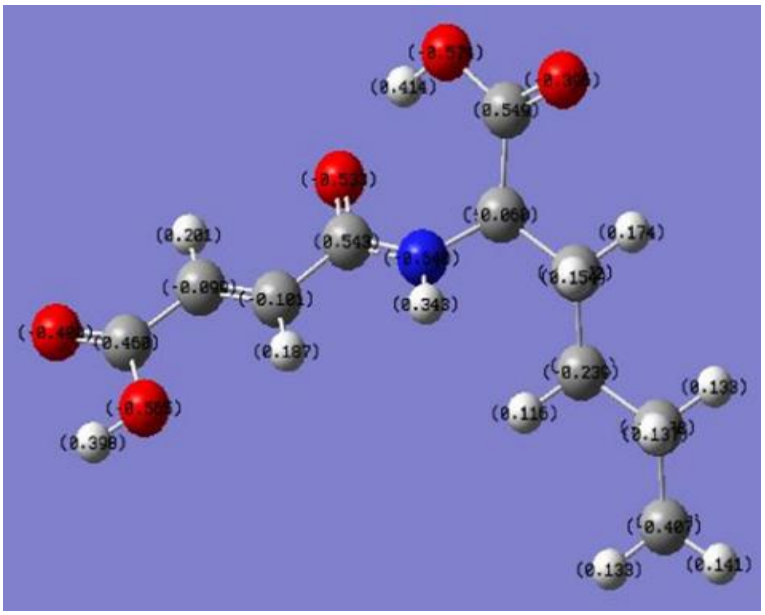

Fig. 3. Molecular structure of DLNM crystal.

3.2 FTIR and FT-Raman spectral studies

The theoretical FTIR spectra of the sample are shown in the Fig. 4. And experimental FTIR spectra are shown in the Fig. 5.

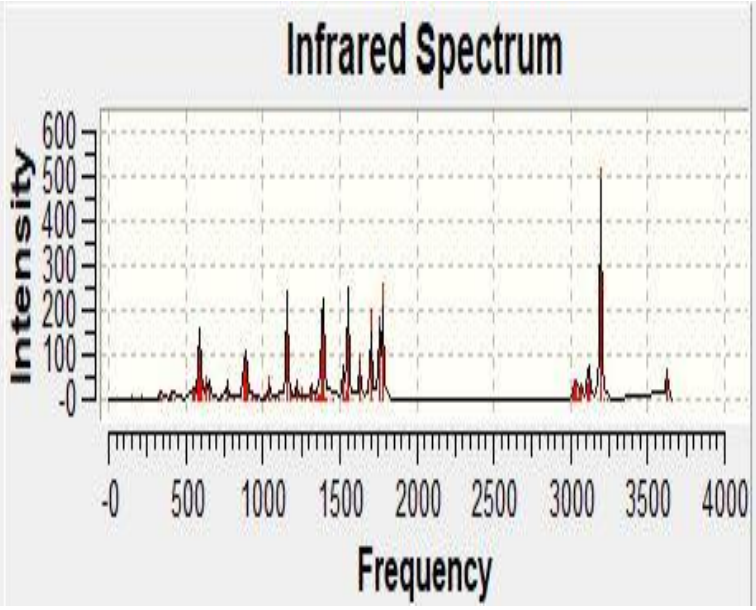

Fig. 4. Theoretical FTIR spectra of DLNM crystal.

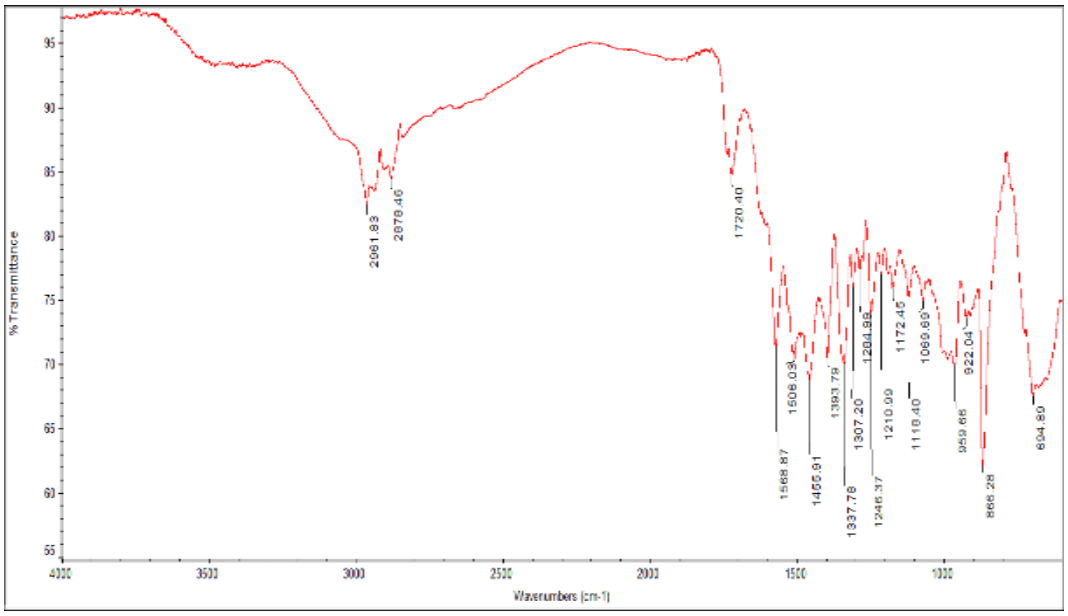

Fig. 5. Experimental FTIR spectra of DLNM crystal.

Some shortcomings can be observed when comparing the experimental and calculated spectral bands. From performed calculations and different conditions take place in the experimental measurements, those spectral bands can results. The theoretical wave numbers calculated agreed well with the experimental bands. The theoretical FT-Raman spectra are given in Fig. 6. And experimental FT-Raman spectrums are given in Fig. 7.

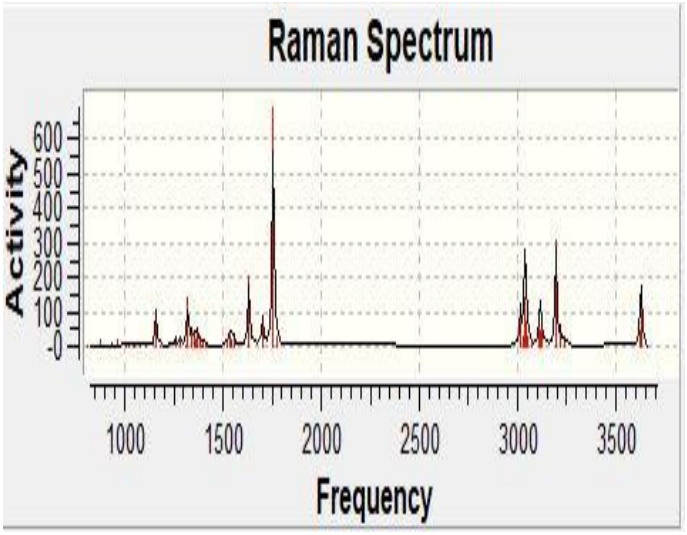

Fig. 6. Theoretical FT-Raman spectra of DLNM.

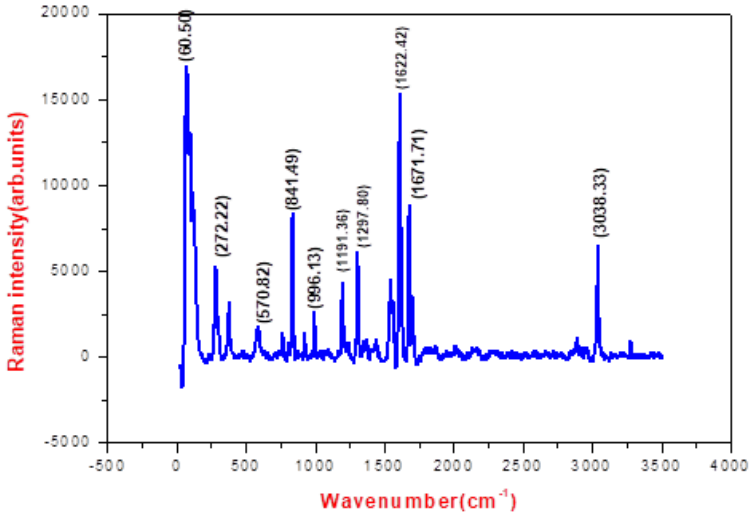

Fig. 7. Experimental FT-Raman spectra of DLNM crystal

The NH_3^+ asymmetric and symmetric stretching band appears at 3999 cm^{-1} and 3085 cm^{-1}, respectively. The C-N stretching vibrations are appeared at 1279 cm^{-1} – 1367 cm^{-1}. The strong and weak bands at 3403 cm^{-1}, and 3153 cm^{-1} are due to asymmetric and symmetric NH_2 vibrations respectively. The asymmetric and symmetric C-H vibration for methyl group indicates at 2975 cm^{-1} – 3149 cm^{-1}. The OH vibration lies in the region 547 cm^{-1} – 694 cm^{-1}. The bands between 1405 cm^{-1} – 1533 cm^{-1} are because of C-C stretching vibrations. The carbonyl absorption owing to C=O stretching vibration is noticed in the range of 1650 cm^{-1} - 172 cm^{-1} [11].

3.3. Thermal studies

The recorded TG/DTA thermal curves of DLNM crystal are shown in the Fig. 8. and it is seen from the figure that the sample has a slight weight loss up to 110 ^oC and this is the first stage and this may be due to liberation of water molecules or moisture in the sample. In the second stage from 120-200^oC, there is about 25% of weight loss of the sample [12-14]. In the third stage from 200-350^oC, there is about 15% of weight loss of the sample. In the fourth stage from 350-600^oC, there is about 25% of weight loss is noticed.

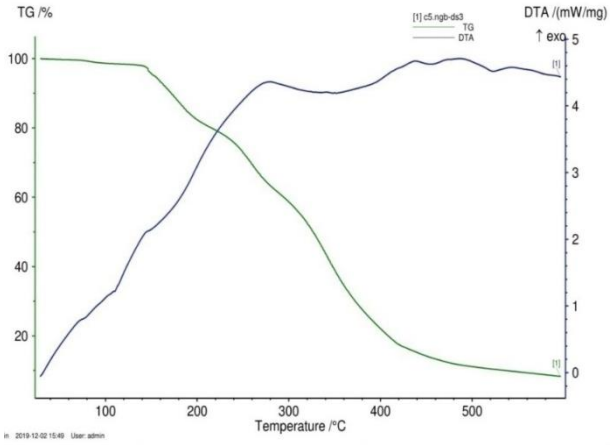

Fig. 8. TG-DTA curve of for DLNM crystal.

The endothermic peaks at 320^{o}C and 400 ^{o}C in the figure show the further decomposition of the sample. The broad exothermic curve from 400^{o}C to 600^{o}C appears due to liberation of gaseous particles from DLNM crystal. Thus, the compound is stable up to 160˚C thermally.

3.4. Mechanical studies

Good quality and well-polished DLNM was laid on the platform of the Vickers micro hardness tester. For considerable amount of various magnitudes were employed for a interval (fixed) of 10 seconds [15-19]. The average diagonal indentation length was measured at different loads for DLNM. Fig. 9 shows the different of hardness along with associated load for DLNM crystal. It is found that the Vickers hardness number of the grown crystal of DLNM, owing to the reverse indentation size effect, increases little by little with increase in load. If the load of above 100 g is applied, cracks form on the smooth surface of the crystal due to release of the internal stresses generated locally by indentation. Using the Meyer's law, $P = ad^{n}$, the value of work hardening coefficient of DLNM crystal was obtained to be 3.0455 (from the Fig.10) which indicates that the material belongs to soft material category [20].

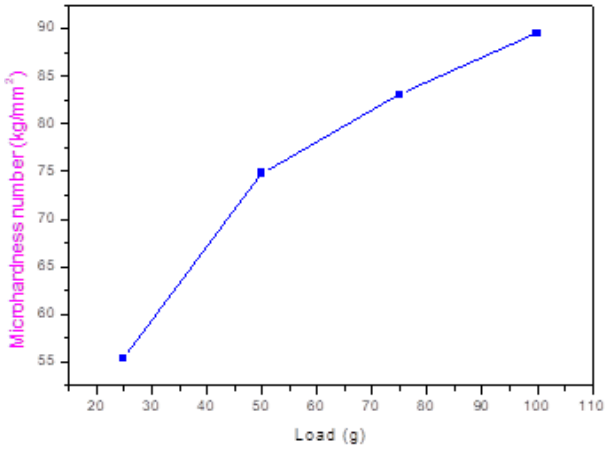

Fig. 9. Plot of hardness number versus d for applied load for DLNM crystal.

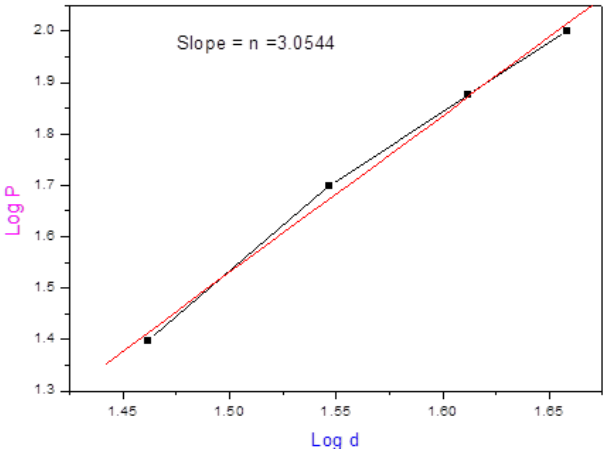

Fig. 10. Plot of log P versus log DLNM crystal.

3.5. Dielectric studies

The dielectric analysis was accomplished at varied temperatures such as 30°C, 50°C and 80°C. The crystals which are silver coating on the opposite laid between the two the two electrodes to set a parallel plate capacitor. The dielectric constant of the material of the crystal, using the relation, was worked out.

$$\varepsilon_r = Ct/A\varepsilon_o$$

where C is the capacitance, A is the area of cross section, ε_o is the permittivity of free space and't' is the thickness of the crystal. The capacitance values of the condenser with or without the dielectric are measured and the dielectric constant was determined. The dielectric loss (tan δ) was found directly using the LCR meter. As a function of varied temperatures, the variation of dielectric constant is shown in the Fig. 11. It, from the graph, is relevant that the dielectric constant decreases progressively for high frequencies.

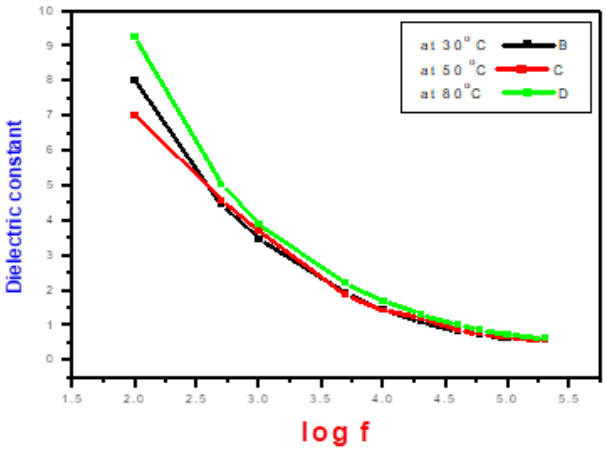

Fig. 11. Variation of dielectric constant frequency for DLNM crystal at different temperature.

The dependency of dielectric constant by means of frequency reveals an identical action for all temperatures. A point is arrived at when the frequency of the engaged field raises. And the space charge can't sustain there.

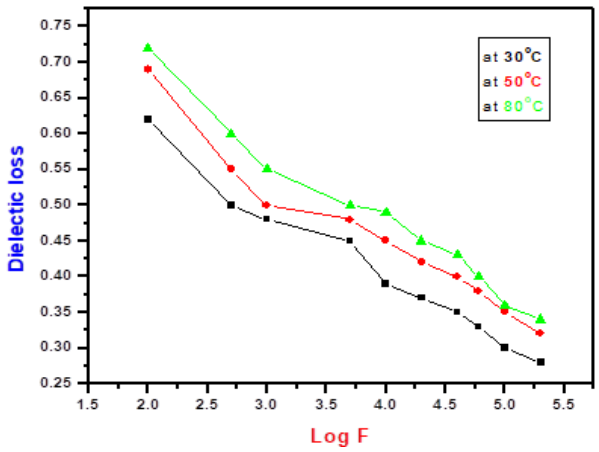

Fig. 12. Variation of dielectric loss with with frequency for DLNM crystal at different temperatures.

Therefore, there is a decrease in the dielectric constant. Hence, decrease of dielectric constant little by little at higher frequencies is attributed to the decline of significance of all the four polarizations. Fig. 12 shows the variation of dielectric loss with frequency. The decrease of both dielectric loss and dielectric constant with the increase of frequency for DLNM crystal is shown by the results [21]. When the temperature of the samples increases, the dielectric parameters are found to be increasing and this is due to the increase of dipole moment and hence polarization in the sample when the temperature is increased. The quality of the grown DLNM crystals is good and it is indicated by low values of dielectric loss. Using the data of dielectric constant and loss factor, the values of AC conductivity (σ_{ac}) for the sample were determined using the equation $\sigma_{ac} = \omega \varepsilon_r \varepsilon_o \tan\delta$, where ω is the angular frequency, ε_r is the dielectric constant, ε_o is the permittivity of free space or vacuum and tan δ is the dielectric loss factor. The variations of AC conductivity with frequency at temperatures such as 30° C, 50° C and 80° C are shown in the Fig. 13.

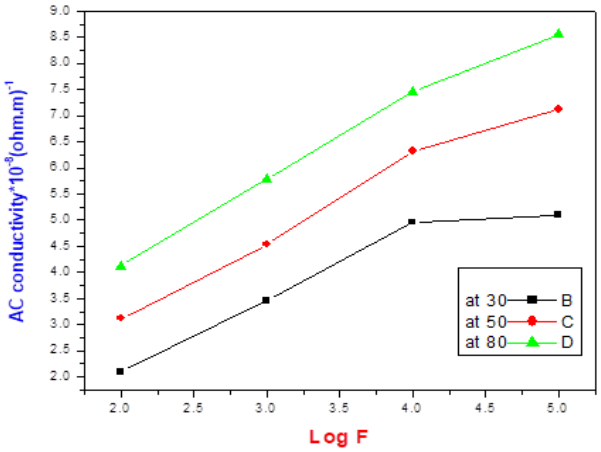

Fig. 13. Plots of AC conductivity versus frequency for DLNM crystal at different temperatures.

3.6. EDAX or EDS spectroscopy

The elemental composition of the crystal is determined from the spectrum of X-ray energy [23-26]. The recorded EDAX spectrum of DLNM crystal is shown in the Fig. 14. The spectra indicates that the element such as C, N, O the grown crystal of DLNM. Since atomic mass of hydrogen is very low, hydrogen cannot be identified by EDAX method.

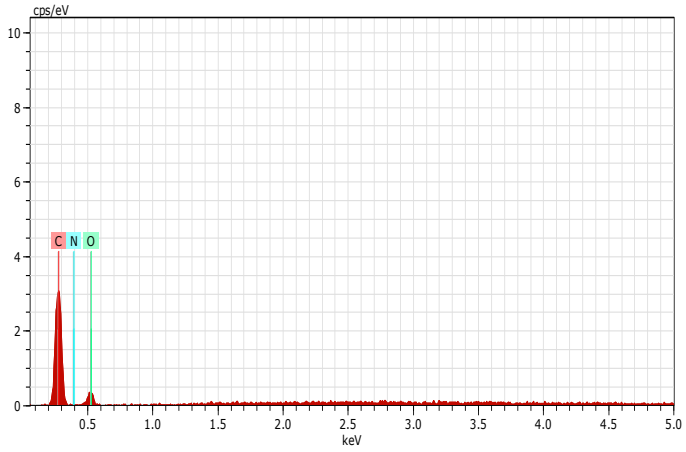

Fig. 14. EDAX spectra of DLNM crystal.

3.7. NMR spectral analysis

The NMR magnetic shielding pattern of the grown DLNM crystal is presented in the Fig. 15. The isotropic chemical shifts δ of ^{13}C and ^{1}H were calculated.

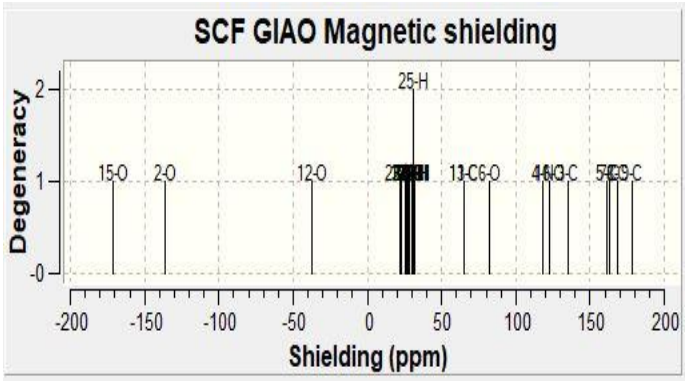

Fig. 15. NMR magnetic shielding pattern of the grown DLNM crystal.

4. Conclusion

Single crystals of DL-Norleucine Maleate (DLNM) were grown by slow evaporation solution growth method. Grown crystals were characterized by Single and Powder X-ray diffraction. The presence of functional groups and the modes of vibration of the molecules, using FTIR and FT-Raman techniques, were identified. Density functional theory (DFT) computation gives optimized structure parameters of DLNM molecule. It is relevant that hydrogen bonds are prevalent in this material. The compound is stably up to 160˚C thermally and it is proved and shown by a TG-DTA thermal study. The Vickers microhardness study leads to the conclusion that the material belongs to soft material category. The dielectric behavior of the sample was studied at different frequencies and temperatures. Various dielectric parameters like AC conductivity, dielectric constant and loss of the sample were determined. EDAX studies identity the different elements that are present in DLNM crystal. NMR spectral and chemical shifts of the grown crystal of DLNM were analyzed.

Acknowledgements

The authors are thankful to the Manonmaniam Sundaranar University, Tirunelveli for rendering the support for the research.

References

[1] D.S. Chemla, J. Zyss, Nonlinear Optical Properties of Organic Molecules and Crystals, Academic Press, New York, 1987.
[2] J. Zyss, J.F. Nicound, M.Coquillay, J. Chem. Phys. 81 4160 (1984); https://doi.org/10.1063/1.448134
[3] I. Ledoux, J. Badan, J. Zyss, A. Migus, D. Hulin, J. Etchepare, G. Grillon, A. Antonetti, J. Opt. Soc. Am. B 4 987 (1987); https://doi.org/10.1364/JOSAB.4.000987
[4] P. Pandi, G. Peramaiyan, M. Krishna Kumar, R, Mohan Kumar, spectrochimica Acta Part A 88 (2012), 77-81; https://doi.org/10.1016/j.saa.2011.11.060
[5] Christian Czech, JurgenGlinnemann, Kristoffer E. Johansson, Michael Bolte, Martin U. Schmidt, ActaCrystallographica Section B, Structural Science, Crystal Engineering and Materials, 2017, Dec 1;73 (pt 6): 1075-1084, doi: 10.1107/S2052520617012057, PMCID: PMC5744409 https://doi.org/10.1107/S2052520617012057
[6] N. Vijayan, G. Bhagavannarayana, R. Ramesh Kumar, R. Gopalakrishnan, K.K. Maurya, P. Ramasamy, Crystal Growth Des., 6, 2006, 1452; https://doi.org/10.1021/cg049594y
[7] S. Natarajan, S. A. Martin Britto, E. Ramachandran, Crystal Growth Des.6 (2006) 137 https://doi.org/10.1021/cg0502439
[8] K. Sambath Kumar, K. Settu, Elixir Vib. Spec. 91, 2016, 38087-38098.
[9] V. S. Kumar, R.S. Sundararajan, Australian Journal of Basic and Applied Sciences, 11(11) August 2017, Pages 132-138.
[10] M. Lakshmi Priya, R. Ezhil Vizhi, D.Rajan Babu, Optik 126 (2015), 4259-4262 https://doi.org/10.1016/j.ijleo.2015.08.126
[11] P. Vinnarasi, M. Victor Antony Raj, J. Madhavan, Materials Today: Proceedings 8 (2019) 492-501; https://doi.org/10.1016/j.matpr.2019.02.143
[12] Wend land, WW, 1974, Thermal methods of Analysis, John Wiley and Sons, New York.
[13] Emadi, D, Whiting, LV, Nafisi, S, &Ghomashchi, R, 2005, J.Thermal Analysis and Calorimetry, vol.81, pp. 235; https://doi.org/10.1007/s10973-005-0772-9
[14] Brown, ME, 1988, Thermal Analysis Techniques and Applications, Chapman and Hall, New York.
[15] K. Sangwal, Mater. Chem. Phys. 63, 145 (2000); https://doi.org/10.1016/S0254-0584(99)00216-3
[16] K. Sangwal, J. Optoelect. Adv. M. **2**, 105 (2000); https://doi.org/10.1002/(SICI)1527-2648(200003)2:3<105::AID-ADEM105>3.0.CO;2-P
[17] B. Wolf, Cryst. Res. Technol. 35, 377 (2000); https://doi.org/10.1002/1521-4079(200004)35:4<377::AID-CRAT377>3.0.CO;2-Q
[18] M.A.Meyer, Some aspects of the hardness of metals, Ph.D. Thesis, Dreft, (1951).
[19] Scaife, B, 1998, Principles of Dielectrics, Oxford University Press
[20] Susmita Karan, S.P. Sen Gupta, Mater. Sci. Eng.,A 398 (2005) 198-203 https://doi.org/10.1016/j.msea.2005.03.016
[21] J.R. Macdonald, Impedance Spectroscopy, Emphasizing Solid Materials and Systems, Wiley Interscience Publ., NewYork, 1987.
[22] R.H. Chen, T.M. Chen, C.S. Shern, J. Phys. Chem. Solids 61 1399 (2001); https://doi.org/10.1016/S0022-3697(00)00019-6
[23] Skoog, 2007, Principles of Instrumental Analysis, Belmont, CA, Thomson Brooks/Cole., Belmont, CA
[24] Severin, P. 2004, Kenneth, Energy dispersive spectrometry of common rock forming Minerals, Kluwer Academic Publishers.
[25] Russ, JC, 1984, Fundamentals of Energy Dispersive X-ray Analysis, Butter worths, London.
[26] Anwar, J.; Tuble, S. C.; Kendrick, J. Am. Chem. Soc., 129, 2542−2547 (2007); https://doi.org/10.1021/ja066686y